Corrosion Resistance of Ornaments Made of Thermo Active Super Elastic Alloy in Artificial Sweat under the Influence of Sodium Chloride and Urea

T. Umamathi[1], R. Parimalam[1], K. Anuradha[1],
B. Mahalakshmi[1], M. J. Jency[2] and S. Rajendran[2*]

[1]Department of Chemistry, Sri Meenakshi Government Arts College for Women (A), Madurai, Tamil Nadu, India
[2]Corrosion Research Centre, Department of Chemistry, St Antony's College of Arts and Sciences for Women (Affiliated to Mother Teresa Women's University, Kodaikanal), Dindigul, Tamil Nadu, India
**Corresponding author:susairajendran@gmail.com*

Received 26/11/2024; accepted 10/03/2025
https://doi.org/10.4152/pea.2027450103

Abstract
Whenever metals or alloys are exposed to sweat, electrolytes present in it corrode them, forming an oxide layer on their surface. This causes several undesirable effects such as corrosion and malfunction. CR of Thermo Active Super Elastic Alloy (TASEA) immersed in artificial sweat (AS) with 100 ppm NaCl and 100 ppm urea was herein investigated and compared by polarization study and AC impedance spectra. It was seen that CR of TASEA immersed in AS with 100 ppm NaCl/urea increased. When TASEA was immersed in AS with 100 ppm NaCl linear polarization resistance (LPR) increased from 1760283 to 9506106 Ohm/cm^2, i_{corr} decreased from 2.382 x 10^{-8} to 4.008 x 10^{-9} A/cm^2, R_{ct} increased from 4884 to 12210 Ohm/cm^2, impedance increased from 4.367 to 4.8, C_{dl} decreased from 10.442 x 10^{-10} to 4.1769 x 10^{-10} F/cm^2 and phase angle increased from 48.1 to 68°. When TASEA was immersed in AS with 100 ppm urea LPR increased from 1760283 to 2430930 Ohm/cm^2, i_{corr} decreased from 2.382 x 10^{-8} to 2.004 x 10^{-8} A/cm^2, R_{ct} increased from 4884 to 10740 Ohm/cm^2, impedance increased from 4.367 to 4.777, C_{dl} decreased from 10.442 x 10^{-10} to 4.748 x 10^{-10} F/cm^2 and phase angle increased from 48.1 to 66°.

Keywords: AC impedance spectra; AS; CR; NaCl, polarization study; TASEA; urea.

Introduction•

Human sweat contains several electrolytes that have essential roles in the body. Na and Cl$^-$ are electrolytes most abundant in sweat, with K, Mg and Ca present in lower amounts. Sweat also contains tiny amounts of metabolites such as lactate, ammonia and urea. It can contact with a number of consumer products and damage

---

•The abbreviations and symbols definition lists are in pages 40-41.

products service life through several unacceptable effects such as corrosion and impairment. CR of several metals and alloys in contact with many body fluids has been studied by several researchers [1-15].

Corrosion behavior of Cu coin materials in the presence of human sweat has been analyzed by [1], with polarization, AC impedance spectra, SEM and EDX studies. Corrosion behavior of brass coinage metal in a AS solution has been analyzed by [2], with electrochemical measurement and surface analysis methods, including SEM and EDX spectrometry. Cl^- in sweat solution has accelerated anodic active dissolution of brass, which causes pitting and dezincification corrosion.

CR of thermo active alloy and 18 K Au alloy immersed in AS with 100 ppm NaCl has been investigated by [3], using electrochemical studies such as polarization study and AC impedance spectra. It has been observed that CR of thermo active alloy and also 18 K Au alloy immersed in AS with 100 ppm NaCl increased. A simple solution-immersion method based on the concept of predesigned corrosion developed to enhance the CR of a Mg-Nd alloy has been reported by [4].

Percutaneous penetration of Be and Cu contained in metallic items as eyeglass temple tips (specifically, BrushCAST® Cu-Be casting alloys containing 0.35 < 2.85% Be and 95.3–98.7% Cu), has been studied by [5], using Franz diffusion cells. This work has demonstrated that total skin absorption of Cu was higher (8.86%) than that of Be (4.89%), which has been expected, based on the high percentage of Cu contained in eyeglass temple tips.

Different body fluids in the presence of different implantation metals and protective films formed have been analyzed by [6], using electrochemical methods and various surface analysis techniques such as AFM, FTIR-UV and SEM. Five typical metal materials for fashion jewelry, including 316L stainless steel, TA2 pure Ti, Co-Cr-Mo alloy, tungsten carbide and tantalum carbide (TaC), have been investigated comparatively for their physical, chemical and mechanical properties, and process and safety performance. The results show that all experimental materials showed highest brightness for Co-Cr-Mo alloy, and highest chromatic value for TaC system. The five metals obtained excellent CR in AS.

Highest E_{corr} for TA2, and lowest for tungsten carbide [7, 8] have explained the CR of thicker praseodymium-rich oxide layer which was obtained on Mg substrate after ion implantation compared to original oxide film. CR in AS has improved, as demonstrated by polarization and immersion tests. The improvement observed for Al-containing Mg alloy was more significant than that on pure Mg.

Differences in Ni and Co release from massive forms of a range of common stainless steels and some high-alloyed grades, compared to Ni and Co metals, have been assessed in AS, for 1 week, at 30 °C [9]. Anti-corrosion of molded interconnect devices in harsh environments, such as in contact with human sweat, is a challenge, since the metals have large differences in electrode potential, and part of the circuitry has been positively polarized during operation.

The first electrochemical numerical simulation for Co-Cr alloy and Ti, with friction in a simulated body fluid, has been performed by [10, 11]. It has been found that current density of both single metal and galvanic coupling metals models has increased with a wider area of non-friction.

CR of Pd- and Au-based alloys in AS has been studied by [12]. 316L stainless steel has been widely used for fashion jewelry, but it can carry a large number of bacteria and bring the risk of infection, since the steel has no antimicrobial performance. The effects of Ce on antibacterial property, CR and processability of 316L have been studied by microscopic observation, thin film adhering quantitative bacteriostasis and electrochemical and mechanical tests.

CR of SS 18/8 and 22 K Au alloys immersed in AS with 100 ppm D-Glucose has been studied by [13, 14], using polarization study and AC impedance spectra. It has been observed that CR of the alloys has decreased. Corrosion behavior of Cu-Fe alloy used as jewelry in synthetic sweat solution has been studied by [15]. Results showed that the sample had negative E_{corr} and highest I_{corr}.

Human sweat can cause a variety of undesirable effects. Constant handling of metal parts by some individuals causes rust accumulation. Many ornaments made of TASEA, such as wrist watches, chains, rings and bangles, may come in contact with sweat, which may contain excess of NaCl and urea. These chemicals, in addition to sweat, may cause TASEA corrosion.

The present work was undertaken to investigate and compare the influence of NaCl and urea on CR of TASEA in AS, by electrochemical studies such as polarization study and AC impedance spectra.

Experimental methods

Preparation of the metal specimens

A thin wire of TASEA was used as a test material for this work. TASEA is mainly composed of 54.52% Ni and 45.48% Ti. It has ultimate tensile strength and elasticity, and it is used in catheters, stents, ornaments, orthodontics for brackets and super elastic needles.

TASEA was encapsulated in a Teflon rod. It was polished to mirror finish and used for electrochemical studies. TASEA was immersed in AS (3160-ISO standard), of which composition was: 20 g/L NaCl, 17.5 g/L NH_4Cl, 5 g/L acetic acid and 15 g/L d,l lactic acid, with pH adjusted to 4.7 by NaOH. In electrochemical studies, TASEA and AS were used as working electrode and electrolyte, respectively. The temperature was maintained at 37 ± 0.1 °C.

Electrochemical study

In the present work, CR of TASEA immersed in various test solutions was measured by AC impedance spectra and polarization study, which carried out in a CHI electrochemical work station/ analyzer, model 660A.

Polarization study

Polarization studies were carried out in a three-electrode cell assembly (Fig. 1). SCE, Pt and TASEA were the reference, counter and working electrodes, respectively. From the polarization study, corrosion parameters such as E_{corr}, I_{corr}, β_a, β_c and LPR values were measured.

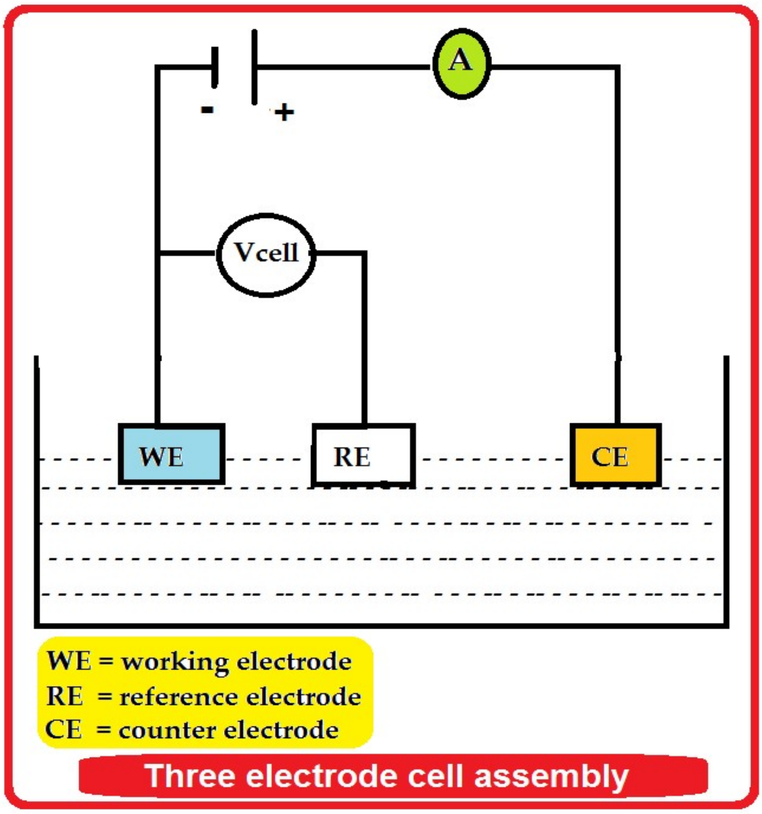

Figure 1: Three electrode cell assembly.

AC impedance spectra

In the present investigation, the same instrument and set-up used for polarization study was also used to record AC impedance spectra. A time interval from 5 to 10 min was given for the system, to attain a steady state OCP. Real (Z') and imaginary (-Z'') parts of cell impedance were measured in ohms, at various frequencies. AC impedance spectra were recorded with initial E(v) of 0, high frequency (Hz) of 1 x 10^5, low frequency (Hz) of 1, amplitude (V) of 0.005 and quiet time (s) of 2. From Nyquist plot, R_{ct} and C_{dl} values were calculated. From Bode plots, impedance and phase angle values were calculated.

Results and discussion

The present investigation was undertaken to study the CR of ornaments made of TASEA in AS with 100 ppm NaCl and 100 ppm urea, by polarization study and AC impedance spectra [16-25].

Influence of NaCl/urea on CR of TASEA immersed in AS

The influence of 100 ppm NaCl and 100 ppm urea on CR of TASEA in AS was investigated by polarization study, of which curves are shown in Figs. 2-4.

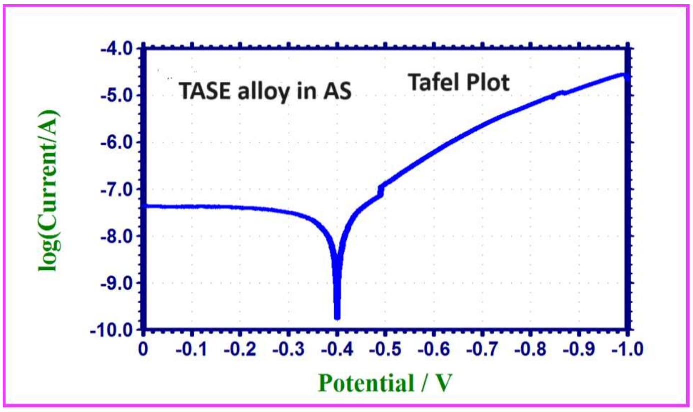

Figure 2: Polarization curve of TASEA immersed in AS.

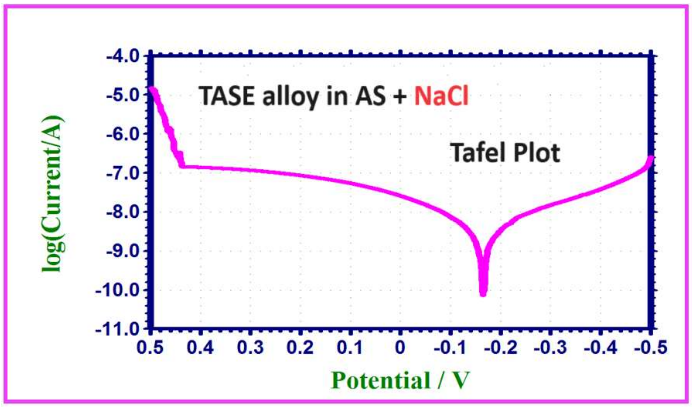

Figure 3: Polarization curve of TASEA immersed in AS + NaCl.

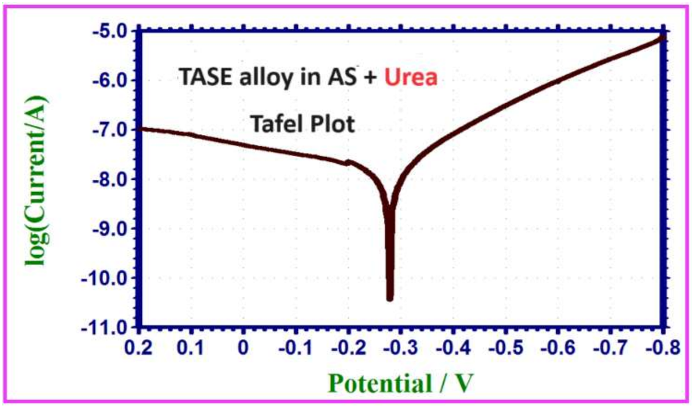

Figure 4: Polarization curve of TASEA immersed in AS + urea.

Corrosion parameters are given in Table 1, and compared in Figs. 5-7.

Table 1: Corrosion parameters of TASEA immersed in various test solutions containing AS, obtained by polarization study.

System	E_{corr} mV/SCE	β_c mV/decade	β_a mV/decade	LPR Ohm/cm^2	I_{corr} A/cm^2
TASEA+AS	-400	90	429	1760283	2.382 x10^{-8}
TASEA +AS	-165	189	164	9506106	4.008x10^{-9}
TASE A+ AS +100 ppm urea	-279	140	564	2430930	2.004 x10^{-8}

When TASEA was immersed in AS with 100 ppm urea, LPR value increased from 1760283 to 2430930 Ohm/cm^2, i_{corr} decreased from 2.382 x 10^{-8} to 2.004 x 10^{-8} A/cm^{-2} and E_{corr} values shifted from -400 to -279 mV *vs.* SCE. It was inferred that, with 100 ppm urea, anodic reaction was predominantly controlled.

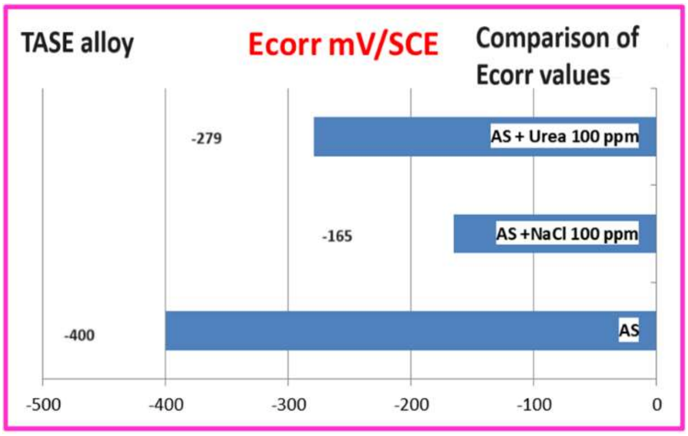

Figure 5: E_{corr} values of TASEA immersed in various test solutions.

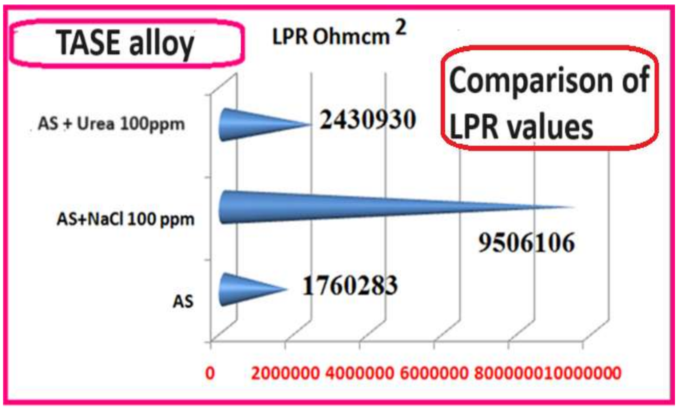

Figure 6: LPR values of TASEA immersed in various test solutions.

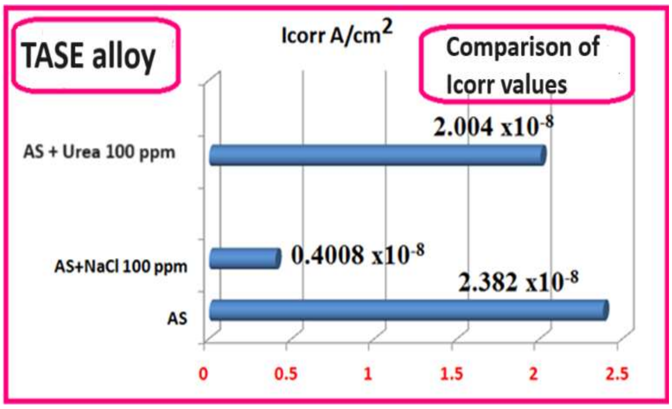

Figure 7: I_{corr} values of TASEA immersed in various test solutions.

Correlation of corrosion parameters of TASEA in AS + NaCl/urea, obtained by polarization study, is shown in Scheme A.

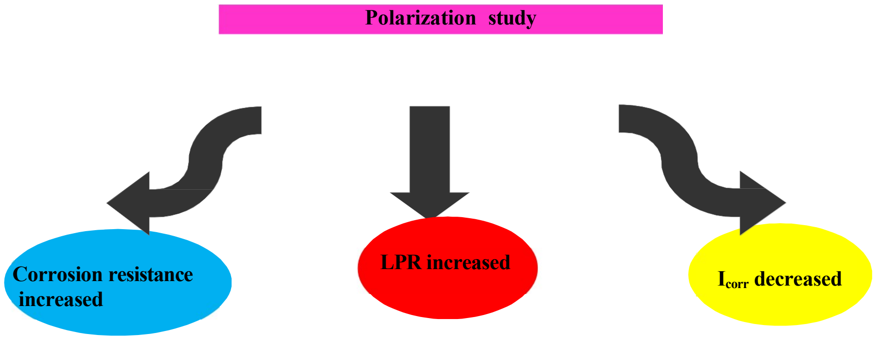

Scheme A: Corrosion parameters of TASEA in AS + NaCl/urea by polarization study.

Implication

CR of TASEA in AS increased with 100 ppm NaCl and 100 ppm urea. Hence, people with excess of NaCl/urea in sweat need not worry about wearing ornaments made of TASEA, such as wrist watches, rings and bangles.

AC impedance spectra

AC impedance spectra of TASEA in AS with 100 ppm NaCl and urea are shown in Figs. 8-16. Nyquist plots are shown in Figs. 8-10.

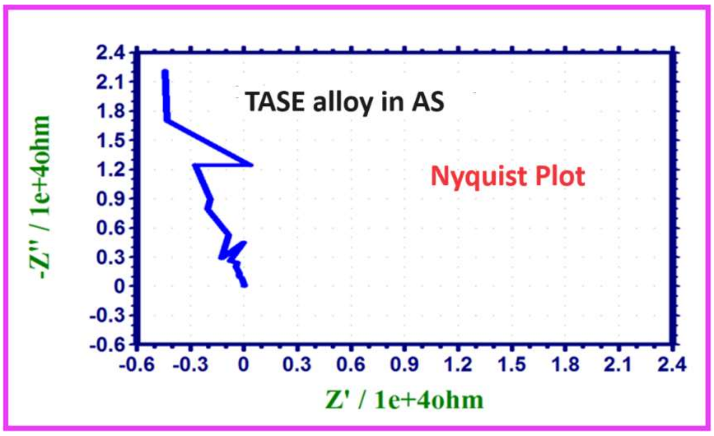

Figure 8: Nyquist plot of TASEA immersed in AS.

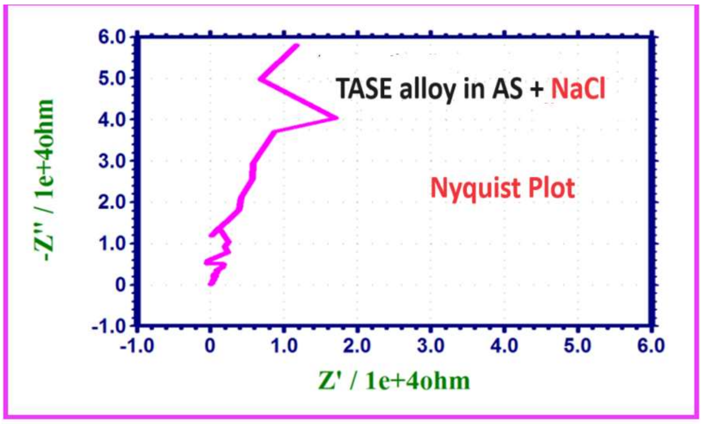

Figure 9: Nyquist plot of TASEA immersed in AS + NaCl.

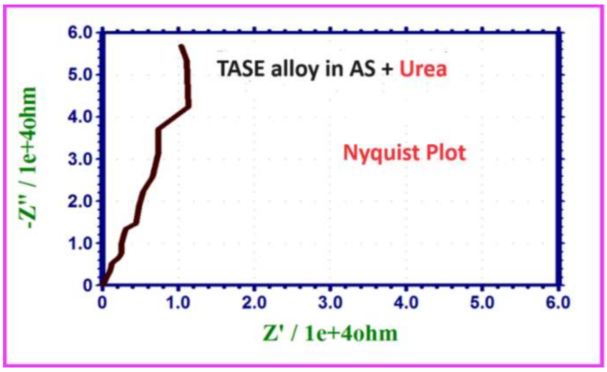

Figure 10: Nyquist plot of TASEA immersed in AS + urea.

Bode plots are shown in Figs. 11-16.

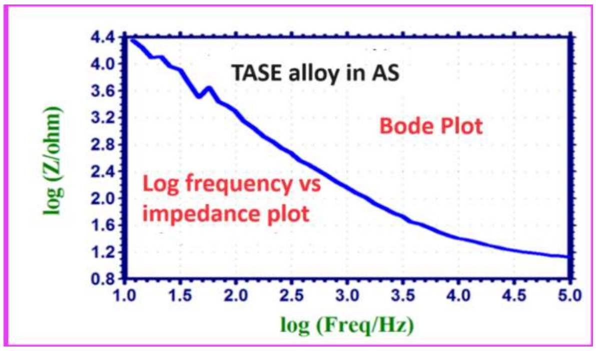

Figure 11: Bode plot (log frequency *vs.* impedance) of TASEA immersed in AS.

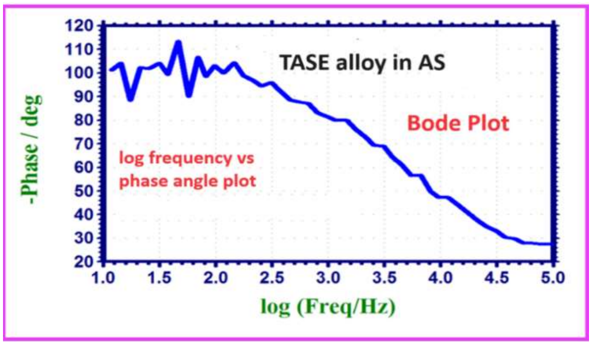

Figure 12: Bode plot (log frequency *vs.* phase angle) of TASEA immersed in AS.

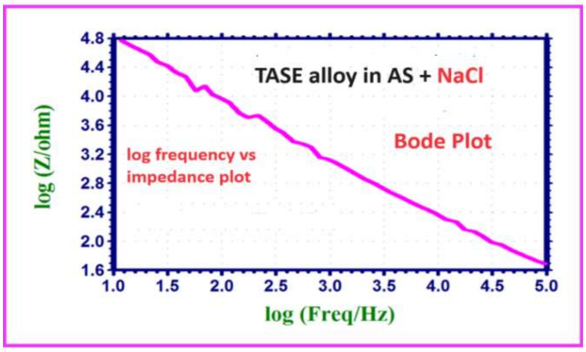

Figure 13: Bode plot (log frequency vs impedance) of TASEA immersed in AS + NaCl.

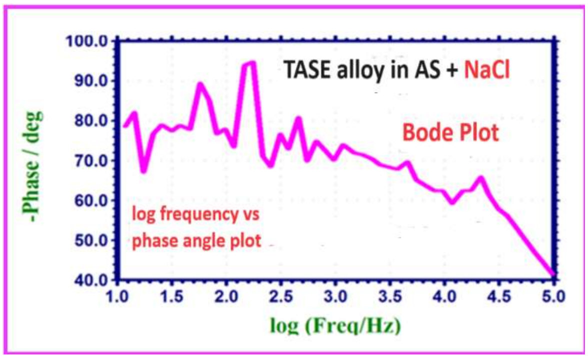

Figure 14: Bode plot (log frequency vs phase angle) of TASEA immersed in AS + NaCl.

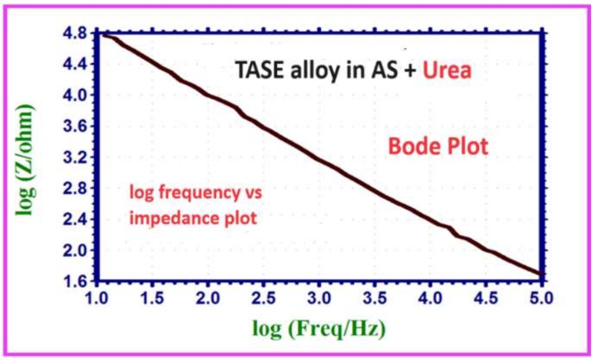

Figure 15: Bode plot (log frequency *vs.* impedance) of TASEA immersed in AS + urea.

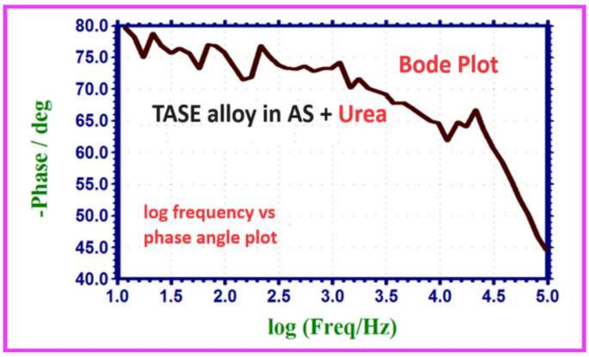

Figure 16: Bode plot (log frequency *vs.* phase angle) of TASEA immersed in AS + urea.

Corrosion parameters are compared in Figs. 17-20.

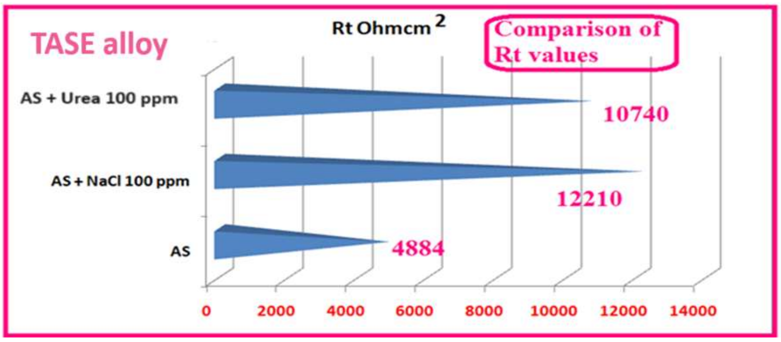

Figure 17: R_{ct} values of TASEA immersed in various test solutions.

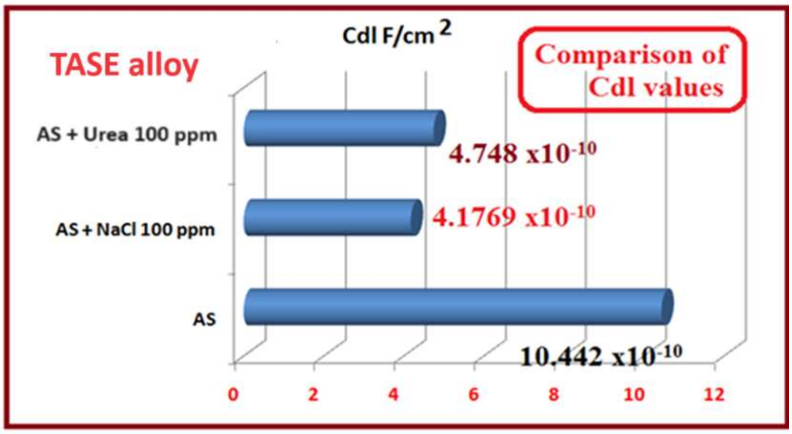

Figure 18: C_{dl} values of TASEA immersed in various test solutions.

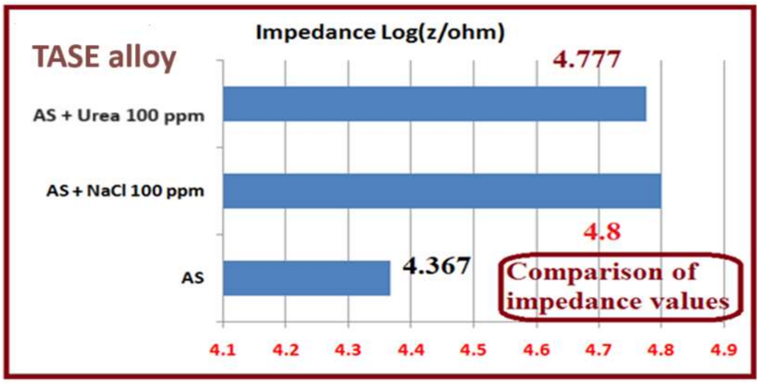

Figure 19: Impedance values of TASEA immersed in various test solutions.

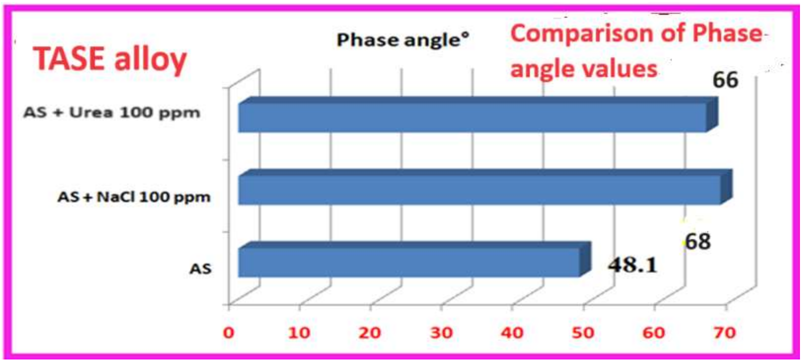

Figure 20: Phase angle values of TASEA immersed in various test solutions.

Corrosion parameters such as R_{ct}, C_{dl}, impedance and phase angle values are given in Table 2.

Table 2: Corrosion parameters of TASEA immersed in various test solutions containing AS obtained by AC impedance spectra.

System	R_{ct} Ohm/cm^2	C_{dl} (F/cm^2)	Impedance log (Z/Ohm)	Phase angle degree
TASE + AS	4884	10.442×10^{-10}	4.367	48.1
TASE + AS+ 100 ppm NaCl	12210	4.1769×10^{-10}	4.8	68
TASE + AS +100 ppm urea	10740	4.748×10^{-10}	4.777	66

Correlation of corrosion parameters of TASEA in AS + NaCl/urea obtained by AC impedance spectra is shown in Scheme B.

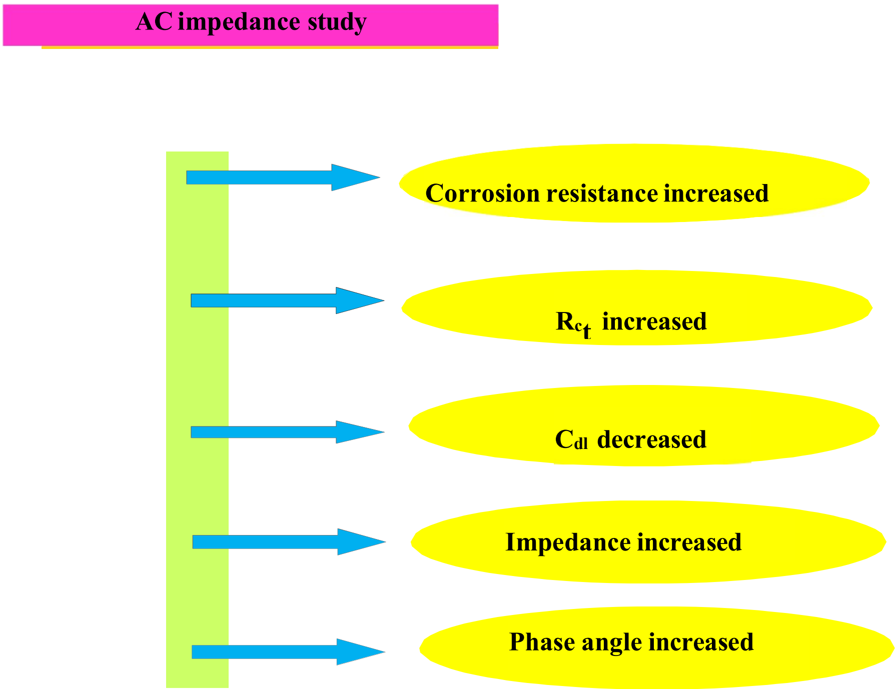

Scheme B: Corrosion parameters of TASEA in AS + NaCl/urea by AC impedance spectra.

Table 2 shows that, when TASEA was immersed in AS with 100 ppm NaCl, R_{ct} value increased from 4884 to 12210 Ohm/cm^2, impedance value increased from 4.367 to 4.8, C_{dl} decreased from 10.442 x 10^{-10} to 4.1769 x 10^{-10} F/cm^2 and phase angle increased from 48.1° to 68°. When TASEA was immersed in AS with 100 ppm urea, R_{ct} increased from 4884 to 10740 Ohm/cm^2, impedance value increased from 4.367 to 4.777, C_{dl} decreased from 10.442x10^{-10} to 4.748x10^{-10} F/cm^2, and phase angle increased from 48.1 to 66°.

Implication

CR of TASEA in AS increased with 100 ppm NaCl and also 100 ppm urea. Hence, people having excess of NaCl/urea in sweat need not worry about wearing ornaments made of TASEA, such as wrist watches, rings and bangles.

Conclusions

CR of TASEA in AS, with NaCl and also urea, was investigated by polarization study and AC impedance spectra. It was inferred that CR of TASEA in AS increased with NaCl and urea. This has been revealed by the increase in LPR, R_{ct}, impedance and phase angle, and by the decrease in i_{corr} and C_{dl} values. Hence, people with excess of NaCl urea in sweat need not worry about wearing ornaments made of TASEA, such as wrist watches, rings and bangles (Table 3).

Table 3: Conclusions of the study.

Corrosion parameters (TASEA)	AS	AS + NaCl (100 ppm) (increased/decreased)	AS + urea (100 ppm) (increased/decreased)
LPR	1760283	9506106 (increased)	2430930 (increased)
R_{ct}	4884	12210 (increased)	10740 (increased)
Impedance	4.367	4.8 (increased)	4.777 (increased)
i_{corr}	2.382×10^{-8}	$4.008 x 10^{-9}$ (decreased)	$2.004 x 10^{-8}$ (decreased)
C_{dl}	$10.442 x 10^{-10}$	$4.1769 x 10^{-10}$ (decreased)	$4.748 x 10^{-10}$ (decreased)
Phase angle	48.1°	68° (increased)	66° (increased)

Acknowledgement
The authors are thankful to the management for their help and support.

Authors' contributions
T. Umamathi, R. Parimalam, K. Anuradha, B. Mahalakshmi and M. J. Jency: conceptualization and validation; review and editing. **S. Rajendran**: writing; correspondence. All authors have read and agreed to the published version of the manuscript.

Abbreviations

AC: alternating current
AFM: atomic force microscopy
AS: artificial sweat
C_{dl}: double layer capacitance
CE: counter electrode
CR: corrosion resistance
E_{corr}: corrosion potential
EDX: energy dispersive X-ray spectrometer
EIS: electrochemical impedance spectra
FTIR: Fourier transform infrared spectroscopy
i_{corr}: corrosion current
ISO: international organization for standardization
LPR: linear polarization resistance
NaCl: sodium chloride
NaOH: sodium hydroxide
NH_4Cl: ammonium chloride
OCP: open circuit potential
ppm: parts per million
R_{ct}: charge transfer resistance
RE: reference electrode
SCE: saturated calomel electrode
SEM: scanning electron microscope
TAC: tantalum carbide
TASEA: thermo active super elastic alloy
UV: ultra violet spectroscopy
WE: working electrode

Symbols definition

β_a: anodic Tafel slope
β_c: cathodic Tafel slope
s: time
V: amplitude
Z': real part of cell impedance
-Z": imaginary part of cell impedance

References

1. Lamiaa MZ, Elzohry AM, Khorshed AL et al. Corrosion Behavior of Coins in Artificial Sweat Solution: A Review. Int J Electrochem Sci. 2022;17:220110. https://doi.org/10.20964/2022.01.17
2. Liang C-H, Wang S-S, Huang N-B et al. Corrosion behavior of brass coinage in synthetic sweat solution. The transaction of nonferrous metals society of China. 2015;25:654-660. https://doi.org/10.1016/S1003-6326(15)63649-4
3. Gowrani T, Anitha N, Dhanalakshmi M et al. Electrochemical studies on the corrosion resistance of 18 K Au and Thermo active alloy in artificial sweat in presence of sodium chloride. Zast Mater. 2023;63:38-47. https://doi.org/10.5937/zasmat2301038G
4. Changyang L, Jiapeng S, Guosong W. Effect of Superhydrophobic Surface on Corrosion Resistance of Magnesium-Neodymium Alloy in Artificial Hand Sweat. Metals. 2023;13:219. http://dx.doi.org/10.3390/met13020219
5. Magnano GC, Marussi G, Adami G et al. Assessment of dermal absorption of beryllium and copper contained in temple tips of eyeglasses. Toxicol Lett. 2022;361:64-7. https://doi.org/10.1016/j.toxlet.2022.04.001
6. Mary SJ, Delinta D, Ajila A et al. Electrochemical behavior of various implantation biomaterials in the presence of various simulated body fluids–an overview. Mater Prot. 2021;62:213-219. http://dx.doi.org/10.5937/zasmat2103213M
7. Yuan J, Chen L, Huang Y. Performance Comparison between Metal Materials for Fashion Jewelry. Tezh Zhuz Ji You Hej/Spec Cast Nonferr Allo. 2017;37:1050-1053.
8. Wang W, Zhang X, Wu G et al. Praseodymium-surface-modified magnesium alloy: Retardation of corrosion in artificial hand sweat. Mat Let. 2016;163:85-89. https://doi.org/10.1016/j.matlet.2015.10.058
9. Wang X, Herting G, Wei Z et al. Bioaccessibility of nickel and cobalt in powders and massive forms of stainless steel, nickel- or cobalt-based alloys. and nickel and cobalt metals in artificial sweat. Regu Toxicol Pharmacol. 2019;106:15-26. https://doi.org/10.1016/j.yrtph.2019.04.017
10. Huang ZH, Zhou YJ, He W. A combination of self-assembled monolayer and hydrophobic conformal coating for anti-corrosion of Cu/NiP/Au 3D circuitry in artificial sweat solution. Surf Coat Technol. 2017;320:126-131. https://doi.org/10.1016/j.surfcoat.2017.01.087

11. Miyabe S, Fujii N, Fujimoto S. Numerical simulation of tribocorrosion of CoCr alloy and Ti with galvanic coupling in simulated body fluid. J Soc Mater Sci. 2020;69:769-774. https://doi.org/10.2472/jsms.69.769
12. Rizzi P, Fiore G, Corazzari I et al. Au based amorphous alloys: Etching effects and nanocrystals formation. Metal Ital. 2011;103:37-41.
13. Yuan J, Li W, Shen K. Study of Ce-modified antibacterial 316L stainless steel. Chin Found. 2012;9:307-312.
14. Anitha N, Prathipa V, Velkannan V et al. Corrosion resistance of SS 18/8 alloy and Gold 22 K alloy in artificial sweat in the presence of D-Glucose. Zast Mater. 2022;63:418-429. https://doi.org/10.5937/zasmat2204418A
15. Naser SA, Hameed AA, Hussein MA. Corrosion behavior of some jewelries in artificial sweat. AIP Conf Proc. 2020;2213:020030. https://doi.org/10.1063/5.0000111
16. Joycee SC, Raja AS, Amalraj AS et al. Inhibition of corrosion of mild steel pipeline carrying simulated oil well water by *Allium sativum* (Garlic) extract. Inter J Corros Scale Inhib. 2021;10:943-960. http://dx.doi.org/10.17675/2305-6894-2021-10-3-8
17. Dorothy R, Sasilatha T, Rajendran S. Corrosion resistance of mild steel (Hull plate) in sea water in the presence of a coating of an oil extract of plant materials. Inter J Corros Scale Inhib. 2021;10:676-699. http://dx.doi.org/10.17675/2305-6894-2021-10-2-13
18. Shanthy P, Thangakani JA, Karthika S et al. Corrosion inhibition by an aqueous extract of *Ervatamia divaricate*. Inter J Corros Scale Inhib. 2021;10:331-348. http://dx.doi.org/10.17675/2305-6894-2021-10-1-19
19. Jessima SJHM, Berisha A, Srikandan SS et al. Preparation, characterization, and evaluation of corrosion inhibition efficiency of sodium lauryl sulfate modified chitosan for mild steel in the acid pickling process. J Molec Liq. 2020;320:114382. http://dx.doi.org/10.1016/j.molliq.2020.114382
20. Belghiti ME, Ouadi YE, Echihi S et al. Anticorrosive properties of two 3,5-disubstituted-4-amino-1,2,4-triazole derivatives on copper in hydrochloric acid environment: Ac impedance, thermodynamic and computational investigations. Surf Interf. 2020;21:100692. https://doi.org/10.1016/j.surfin.2020.100692
21. Prabha AS, Kavitha K, Shrine HB et al. Inhibition of corrosion of mild steel in simulated oil well water by an aqueous extract of *Andrographis paniculata*. Ind J Chem Technol. 2020;27:452-460. http://dx.doi.org/10.13005/OJPS06.01-02.07
22. Praveena JJM, Clara JA, Rajendran S et al. Inhibition of corrosion of mild steel in well water by an aqueous extract of soapnut (*Sapindus trifoliatus*). Mater Prot. 2021;62:277-290. https://doi.org/10.5937/zasmat2303340S

23. Jeslina VM, Kirubavathy SJ, Al-Hashem A et al. Inhibition of corrosion of mild steel by an alcoholic extract of a seaweed *Sargassum muticum*. Mater Prot. 2021;62:304-315. https://doi.org/10.5937/zasmat2303340S
24. Al-Nami SY, Fouda AS. Corrosion inhibition effect and adsorption activities of methanolic myrrh extract for Cu in 2 M HNO_3. Inter J Electrochem Sci. 2020;15:1187-1205. https://doi.org/10.20964/2020.02.23
25. Christy CMA, Jeyasundari J, Nazeera BVR et al. Corrosion behavior of orthodontic wires in artificial saliva with presence of beverage. In Nanotechnology in the Beverage Industry: Fundamentals and Applications: Chapter 16. 2020;471-504. https://doi.org/10.1016/B978-0-12-819941-1.00016-X